On the possibility of fast neutral production of the inner Io torus

M. M. Cowee and C. T. Russell
Institute of Geophysics and Planetary Physics, University of California, Los Angeles, California, USA

Y. L. Wang
Space and Atmospheric Sciences Group, Los Alamos National Laboratory, Los Alamos, New Mexico, USA

D. A. Gurnett
Department of Physics and Astronomy, University of Iowa, Iowa City, Iowa, USA

Received 9 July 2004; revised 10 April 2005; accepted 31 May 2005; published 3 September 2005.

[1] The Galileo spacecraft passed through the Io torus and its inner boundary on 7 December 1995 and 5 November 2002 during the J0 and A34 passes, respectively. Electron densities inferred from plasma wave measurements on both passes indicated a steep gradient at the inner boundary of the cold Io torus located between 4.5 and 5 R_J (Io is at 5.9 R_J), as well as the expected much less steep gradient in the outer torus, with an outer boundary at distances greater than 8 R_J. We attempt to model the inner torus with the fast neutral production model of Wang et al. (2001). A reduced ion pickup velocity at Io can prevent fast neutrals from penetrating inside the observed inner edge of the cold torus. Outward radial convection that increases with radial distances enables a steady state to be maintained. Differences between the passes are not entirely explained by varying pickup velocity at Io and convective transport. Factors including variable mass loading, diffusive transport mechanisms, dawn-dusk torus asymmetry, and spacecraft trajectory effects may also be important.

Citation: Cowee, M. M., C. T. Russell, Y. L. Wang, and D. A. Gurnett (2005), On the possibility of fast neutral production of the inner Io torus, *J. Geophys. Res.*, *110*, A09205, doi:10.1029/2004JA010678.

1. Introduction

[2] Sulfur monoxide and sulfur dioxide ion cyclotron waves have been detected by the magnetometer on the Galileo spacecraft at distances as far as ~20 Io radii outward and to a lesser extent inward of Io. This ion cyclotron wave production region far exceeds the bounds of the region in which newly born ions should be created in Io's exosphere. These ions should simply be convected downstream from Io with the corotational flow in a wake about 1 Io diameter wide. *Wang et al.* [2001] explained how the ion production region could spread downstream of Io by a multistep ion acceleration and transport process. This process begins with the ionization of Iogenic atmospheric neutrals via photoionization and impact ionization. It is followed by reneutralization via charge exchange near Io and finally reionization far from Io (Figure 1). In the period between step 1 and step 2 the ion experiences the $-\mathbf{v} \times \mathbf{B}$ electric field and is accelerated in Io's rest frame up to twice the local plasma velocity (114 km/s if the ion sees the full corotational velocity). Step 2 allows the neutralized ion to travel freely across field lines to distances far from Io where after step 3 it rejoins the plasma torus and emits cyclotron waves.

[3] *Wang et al.* [2001] applied this process to sulfur monoxide ions for varying ionization, neutralization, and dissociation lifetimes. They showed the overall shape of the resulting ion distribution and the distances to which the neutrals could travel in the gravity fields of Jupiter and Io after the stage of ion acceleration. After the neutral is ionized, no further radial transport occurs in the model. Model runs indicated that Iogenic particles cannot approach arbitrarily close to Jupiter. There is an inner edge to the emplaced particles, whose location depends on the velocity of the background plasma flow near Io, where the particle was first ionized. Further, the density at the inner edge is low.

[4] Plasma densities determined from the Voyager (1979) and Galileo (1995 and 2002) passes through the Io plasma torus are plotted in Figure 2. The Galileo data are from the plasma wave spectrometer, and the Voyager data are from the plasma science instrument. The density profiles show several interesting features. First, there is a drop in local density by a factor of 2–3 in the cold torus about 0.1–0.3 R_J inside the orbit of Io. We attribute this to the details of the convective flow of newly picked up ions at Io rather than the fast neutral transport and do not attempt to explain this feature further. Second, the Galileo electron density profiles on passes J0 and A34 show a steep inner edge and a very steep drop in density. Since the Voyager spacecraft went in to only 4.9 R_J, it is possible that it did not reach the steep density gradient. While the steep gradients observed

0148-0227/05/2004JA010678$09.00

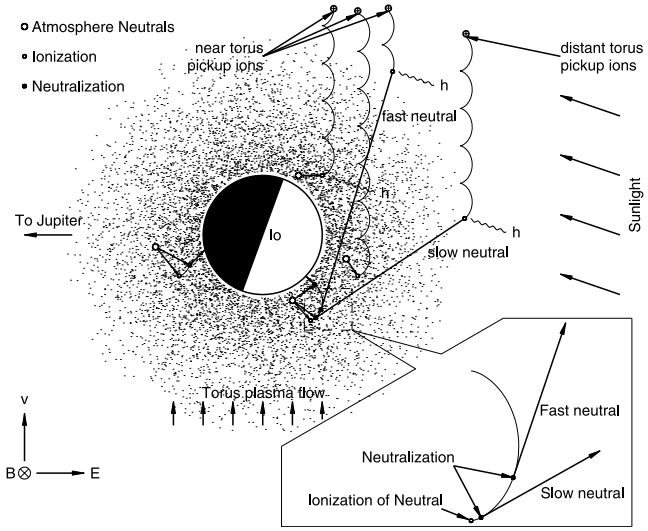

Figure 1. The three-step mechanism proposed to transport mass-loaded ions far from Io [*Wang et al.*, 2001]. Atmospheric neutrals (circles) are ionized in the atmosphere and accelerated by the corotation electric field. Then they are neutralized (dots) by charge exchange and travel across field lines away from Io. Finally, they are reionized (circles) and rejoin the torus plasma, emitting ion cyclotron waves. In the model, ions are picked up into the torus at an altitude of 300 km above the surface of Io with a velocity of 57 km/s (torus corotation velocity minus Io orbital velocity). Characteristic lifetimes for each of the ionization and neutralization stages are 20 gyroperiods (1.6 s gyroperiod for SO^+) for the initial ion lifetime, 1000 gyroperiods for the neutral lifetime, and 500 gyroperiods for the final ion lifetime.

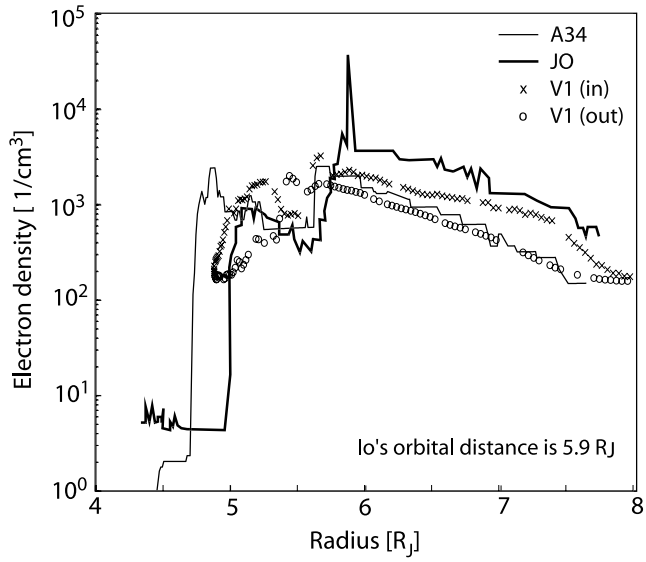

Figure 2. Electron density profiles from the Voyager and Galileo J0 and A34 passes. Voyager plasma science instrument data from the inbound (crosses) and outbound (circles) are shown. Galileo plasma wave spectrometer data from the A34 (thin line) and J0 (thick line) are shown. The J0 pass is a combination of the outbound (8 to 5.4 R_J) and inbound (inside 5.4 R_J) data (adapted from *Bagenal et al.* [1997]). A34 electron densities inferred from the cutoff frequencies (upper hybrid frequency from 8 to 4.9 *Rj* and electron plasma frequency inside 4.9 *Rj*) are courtesy of D. A. Gurnett (private communication, 2003). Only those densities with high certainty were used.

by Galileo are similar in sharpness, they are about 0.3 R_J apart. If we assume Voyager was just outside of the steep gradient, then it would be located between the two Galileo profiles. Both Galileo profiles have a local peak density at a radial distance about 0.2 R_J farther out than the inner edge of the torus (the Voyager density peaks are more difficult to interpret).

[5] Figure 3 shows an example of the *Wang et al.* [2001] simulated two-dimensional (2-D) distribution of fast neutrals. The modeled particles are launched uniformly around Io from an exobase altitude of 300 km. The particles are assigned lifetimes for each of three stages: initial ion, neutral, and final ion. They are influenced only by electric and magnetic forces and gravity during the course of the simulation and can be lost if they travel into Io or Jupiter or outside of the simulation region (>12 R_J from Jupiter). Ions are picked up at Io from an initial velocity of 17 km/s (Io's orbital velocity) into a plasma flow moving at 74 km/s (torus corotation velocity at 5.9 R_J) resulting in an ion pickup velocity, $\mathbf{v}_{\text{pickup}}$, of 57 km/s. This assumes that plasma flowing adjacent to Io's atmosphere, into which newly ionized particles are added, is moving at the same velocity as the corotating plasma. The inner edge of the neutral particle region forms a distinct arc from Io into about 3.4 R_J. Ions will be produced everywhere these fast neutrals penetrate, and then they will drift on constant magnetic field surfaces, which, in the model, are paths at constant distances from Jupiter.

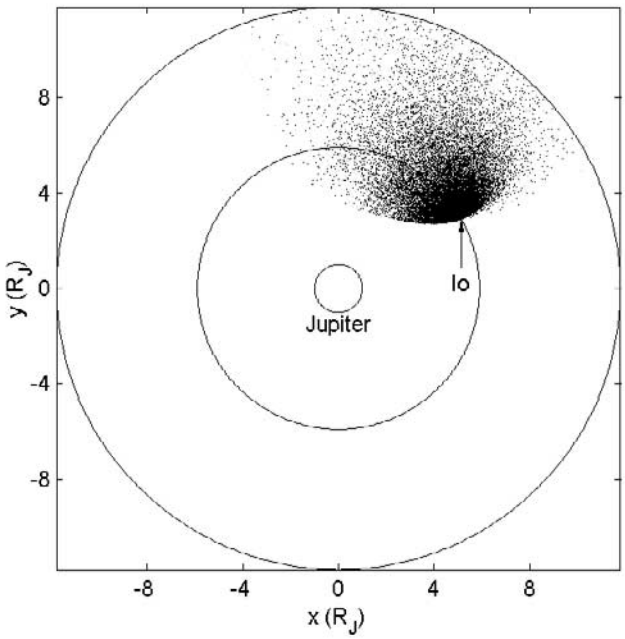

Figure 3. Steady state neutral particle distribution at t = 3.48 hours from the *Wang et al.* [2001] model. Ion pickup velocity is 57 km/s.

[6] Differences between the model radial density profile and the Galileo-measured A34 profile are shown in Figure 4. The modeled inner torus boundary is closer to Jupiter, there is no inner torus boundary drop-off, and there is only a single peak. In addition, the peak is centered at Io's orbital distance not inside it. It may be relevant that this density profile was obtained some distance from Io and not on an Io flyby such as J0. We seek herein to reproduce the inner and outer torus density gradients and the boundary location with our model, but we leave the multiple density peak structure for future work. In order to model the inner boundary drop-off we have coupled the *Wang et al.* [2001] model with a simple 1-D convection (advection) model in which a radially outward velocity profile is applied to its steady state modeled ion distribution. This 1-D model does not include any heating or cooling or ion dissociation processes; ions are lost from the simulation only by exiting the simulation region ($x > 12\ R_J$). The outward, centrifugal motion of the plasma by flux tubes or other mechanism is supported by observational evidence and inferences of outward radial velocities in the torus. Assuming a 1 t/s mass-loading rate, *Russell et al.* [2000] estimated outward radial velocities between 6 and 7 R_J to be about 9 m/s. *Intriligator and Miller* [1982] estimated the velocity to be ~400 m/s near Europa's orbit (~10 R_J). Such outward motion of ions is necessary to maintain a steady state magnetodisk.

2. Results and Discussion

2.1. Inner Torus Boundary Location

[7] As it travels by Io, the background torus plasma is decelerated upstream of the moon and accelerated downstream of it [*Frank et al.*, 1996; *Frank and Paterson*, 2000, 2001, 2002]. For example, when Galileo flew over the Io polar region with a closest approach of 200 km altitude, it detected decreases in the bulk plasma flow speeds from the corotational values to several kilometers per second relative to Io [*Frank and Paterson*, 2002]. An ion picked up into a

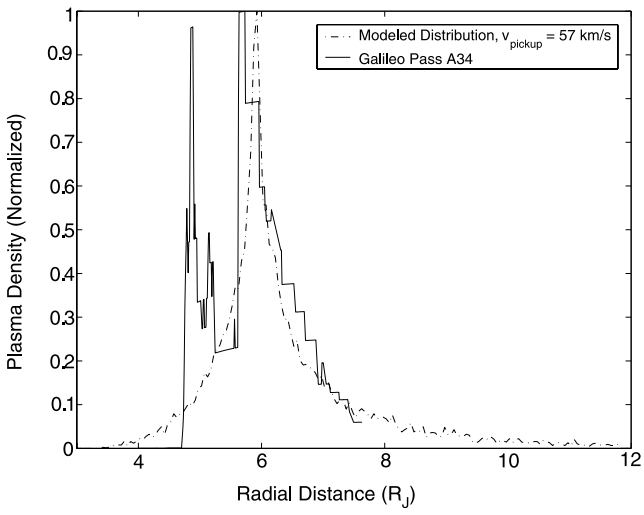

Figure 4. Comparison of the A34 pass (solid line) and the modeled ion distribution with ion pickup velocity equal to 57 km/s (dash-dotted line). A34 data are courtesy of D. A. Gurnett (private communication, 2003).

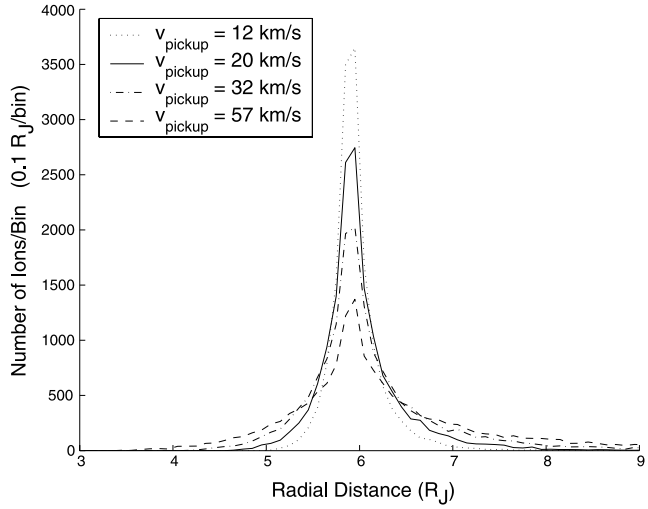

Figure 5. Comparison of the modeled radial distributions of ions for various pickup velocities. The 57 km/s pickup velocity assumes that the ions are picked up at Io's orbital velocity (17 km/s) into a torus plasma flowing at corotation velocity (74 km/s).

plasma with a decreased flow speed will gain less energy because of the lower pickup velocity, $\mathbf{v}_{\text{pickup}} = \mathbf{v}_{\text{flow}} - \mathbf{v}_{\text{ion}}$. In the *Wang et al.* [2001] model this pickup ion then becomes a neutral retaining its velocity and traveling across field lines until it is reionized. The momentum of these fast neutrals derives from the momentum of the pickup ion distribution, which is directly determined by the pickup velocity at Io. Thus ions with lower pickup velocities will not travel as far in their neutral lifetimes as their counterparts with higher pickup velocities. It is then possible that the location of the inner torus boundary is determined by the ion pickup velocity at Io. Figure 5 shows the modeled radial distributions of ions for various ion pickup velocities. With an ion pickup velocity of 57 km/s the ions can attain distances as close as ~3.5 R_J. Decreasing the pickup velocity to 20 km/s moves the inner boundary to ~4.7 R_J, where it was detected on A34. Further deceleration of the plasma flow around Io, producing a pickup velocity of 12 km/s in the charge exchange region, moves the boundary to 5 R_J, consistent with J0.

[8] Figures 6 and 7 show that in addition to altering the boundary locations the ion gyrokinetic temperatures are also affected. The lower ion temperatures are more consistent with the Galileo and Voyager measurements; however, they are still higher than the observed thermal populations of O^{++}, O^{+}, S^{++}, and S^{+} near Io, with temperatures of approximately 30 eV, 30 eV, 90 eV, and 90 eV, respectively [*Frank and Paterson*, 2001]. The modeled average ion temperatures shown in Figure 6 do not agree with these values because the model does not include any ion cooling nor does it consider lower temperatures resulting when sulfur monoxide dissociates into its constituent ions. For all pickup velocities the inner torus is cooler than the outer torus. Figure 7 shows all the ion temperatures versus radial distance. There is a distinct low-temperature "gap" formed as the pickup velocity nears smaller values. This is explained by examining Figure 8, which shows the velocity space of the ions before (large dots) and after (small dots)

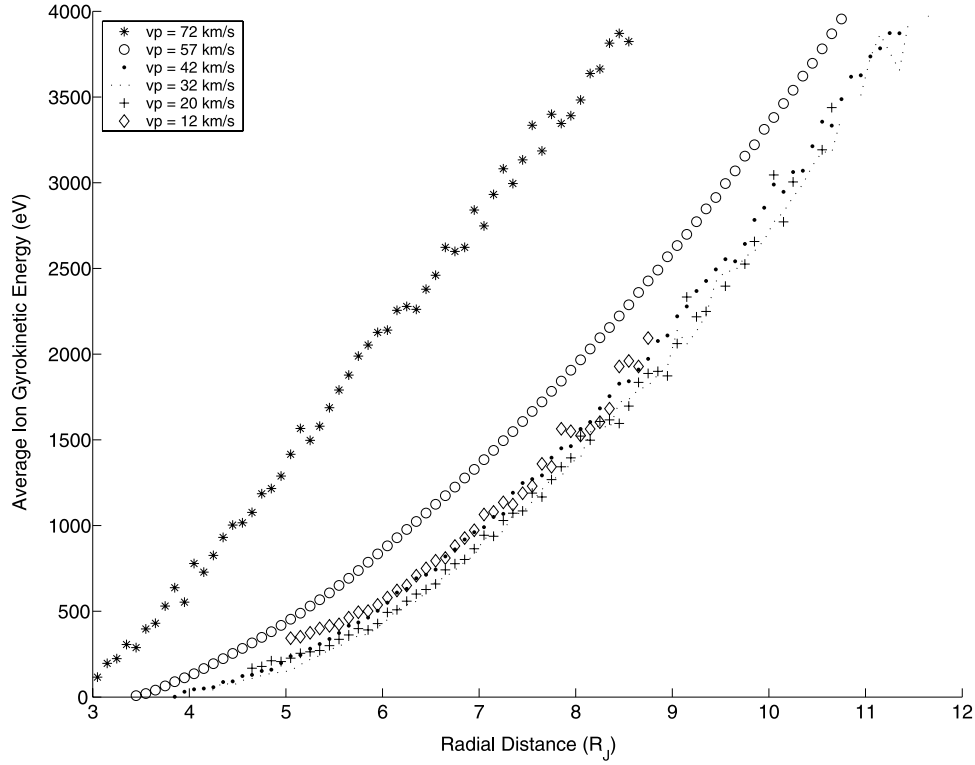

Figure 6. Comparison of the average ion gyrokinetic energies for various pickup velocities. The gyrokinetic energy is the perpendicular energy in the corotating reference frame.

they were accelerated during their final ion lifetime. Before they are accelerated, the ions form ring beams in velocity space in the reference frame of the initial flow field into which they were picked up at Io. However, at distances further from Io, where the reference frame is that of corotational drift, their distribution is restricted (large dots). This restriction shapes the ring beam formed after acceleration (small dots) and prevents ions from having lower velocities.

[9] As shown in Figure 5, the radial profile of the ion density changes shape as the ion pickup velocity is decreased. The ions stay closer to their source, increasing the size of the peak at Io and decreasing the radial extent of the distribution. At the inner and outer torus boundaries the gradients remain relatively the same. The steep drop-off in plasma density at the inner edge of the torus observed by Galileo is likely not a product of the pickup conditions at Io. It is necessary to include other mechanisms to alter the modeled torus density gradients. The outward radial convection of ions, as described in section 2.2, will be shown to further alter the distribution.

2.2. Inner Torus Boundary Gradient

[10] Estimated outward radial convective velocities for Jupiter's magnetodisk from *Russell et al.* [2000] are used as a starting point. We extrapolate the *Russell et al.* [2000] values to the inner torus because although there are plasma pressure gradient forces at work inside Io's orbit, the plasma is so cold that the centrifugal force will dominate, and the net motion of plasma will be outward. The outward radial velocities used are small with respect to the corotation velocity and the ion gyrovelocities, such that a simple 1-D model provides the easiest way to examine the effects of this slow outward convection. The 1-D model solves the mass conservation equation,

$$\frac{\partial n}{\partial t} + \nabla \cdot (n\mathbf{v}) = S,$$

where n is the density, t is time, $\mathbf{v}$ is the convective velocity, and S is the mass-loading source rate (constant). We use the second-order upwind finite difference and Lax-Wendroff schemes to obtain the time evolution of the radial density from this equation. The mass-loading profile is taken from the *Wang et al.* [2001] steady state distribution. For this study, we model outward convective velocities, which are continuous and do not decrease with radial distance.

[11] Figure 9 shows the 57 km/s pickup velocity radial density profiles resulting from the applied outward radial velocity profiles for cases A–C. Applied velocity profile A is a fit from the *Russell et al.* [2000] values and results in an ion distribution, which is peaked at Io's orbit and decays more gradually in the outer torus than near the inner torus boundary. The inner torus boundary is steeper than it would be without radial convection, but it is not as steep as that observed on A34. Also, because of the small velocities and the peaks and valleys of the density-loading profile derived from the *Wang et al.* [2001] model, the steady state convected density profile is not smooth in the inner torus. It is important to note that density values from the model should not be compared directly with observations for several reasons: First, the *Wang et al.* [2001] model did not attempt to mimic measured densities, as its goal was to investigate the shape and extent of the ion distribution only. Second, the ion-loading profile used in the one-dimensional simulation

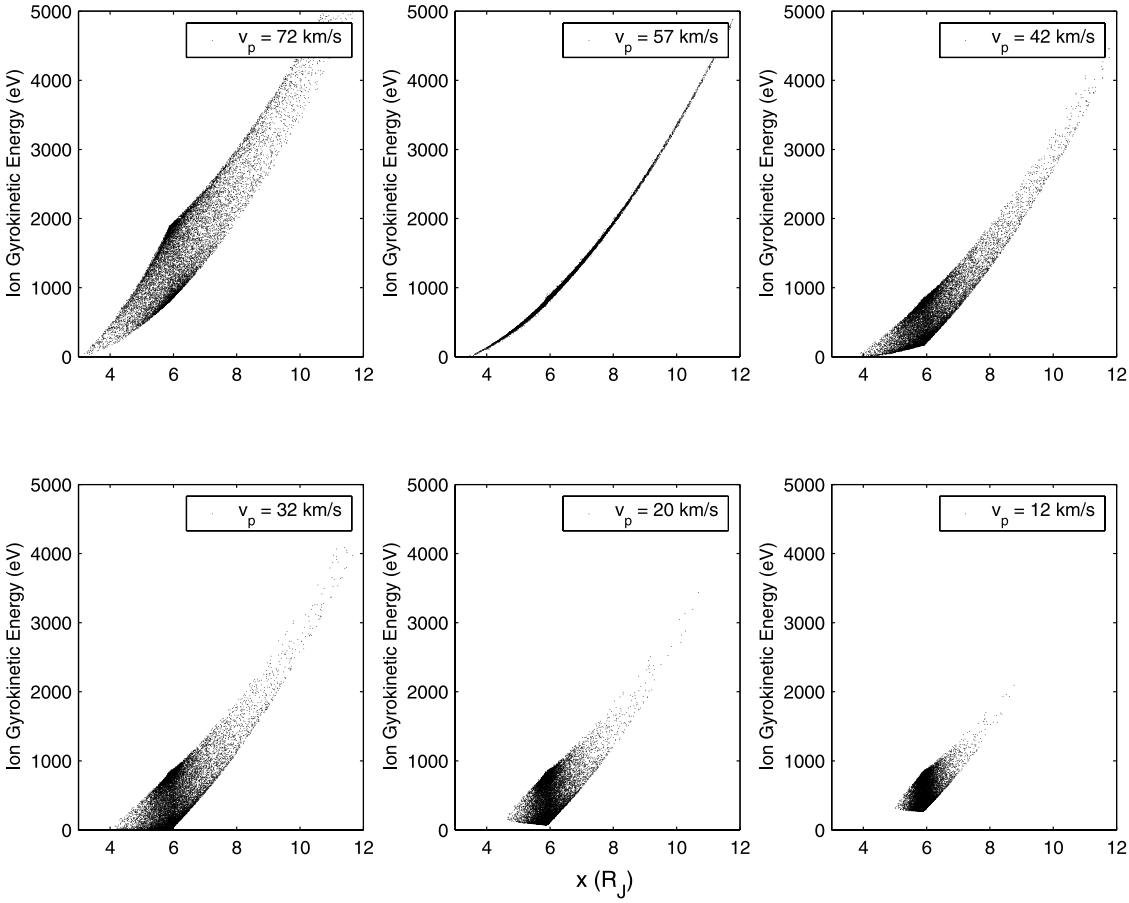

Figure 7. Comparison of all ion gyrokinetic energies versus radial distance for various pickup velocities ($\mathbf{v}_{\text{pickup}}$).

was derived from a two-dimensional simulation. Third, the one-dimensional simulation does not include any ion loss processes. Fourth, the model does not account for the changing volume of an element of plasma as it moves outward in the actual three-dimensional geometry. Also, for these reasons the time required to reach steady state in the simulation is not an estimate of the real values in the torus.

[12] Because simulation A did not have the desired inner torus gradient, other velocity profiles are applied. Velocity profile B rises from 0 m/s at 3.5 R_J to 1000 m/s at Io and is then constant. The resulting ion distribution does not have a steep inner torus boundary, does not peak at Io, and has very high densities out to the end of the simulation region. The extension of the torus density outward from Io is a result of the constant radial velocity, such that in the real torus the velocity likely varies with distance in the outer torus. Velocity profile C is linear across the simulated region (3.5 to 12 R_J), starting at a velocity of 0 m/s at 3.5 R_J and rising to 400 m/s at 12 R_J. The resulting ion profile is peaked at Io and decreases more gradually in the outer torus than in the inner torus. Yet the decreases are both too gradual compared to observations. Increasing or decreasing the slope of the linear velocity profile changes the magnitude of the ion density but leaves the overall shape of the distribution unchanged. It seems that to produce a simulated ion density profile resembling observations, it is necessary to include an outward radial velocity, which increases with distance across the torus. This is consistent with observations that show higher convective velocities at greater radial distances [*Russell et al.*, 2000; *Intriligator and Miller*, 1982]; however, the exact form of the velocity profile is unknown, as it results from nonlinear effects such as variable mass loading in the torus and line tying in the Jovian ionosphere. Thus the simulation work shown next aims at reproducing the observed densities in the torus using simple functional forms of a smooth, continuous, and radially increasing velocity profile.

[13] Using the case of ion pickup at 20 km/s with inner torus boundary at 4.7 R_J, several outward radial velocity profiles are explored. Figure 10 shows the resulting ion and applied velocity profiles for simulations D–G. Velocity profile D is the same as A, but now it is applied to the case of ion pickup at 20 km/s. The results show that the ion distribution is again peaked at Io and decreases gradually away from Io. While the inner torus density gradient remains relatively unchanged despite the outward radial convection of ions, the outer torus has been extended to greater radial distances, decreasing the outer torus gradient. For better agreement with the Galileo A34 data it is necessary to have a velocity profile that allows ions time to build up at the inner torus edge and then rises to values high enough to move the ions out quickly and prevent a buildup in the far outer torus.

[14] Velocity profile E rises more steeply and has a velocity at the inner torus edge half that of D. This profile succeeds in moving particles quickly through the outer

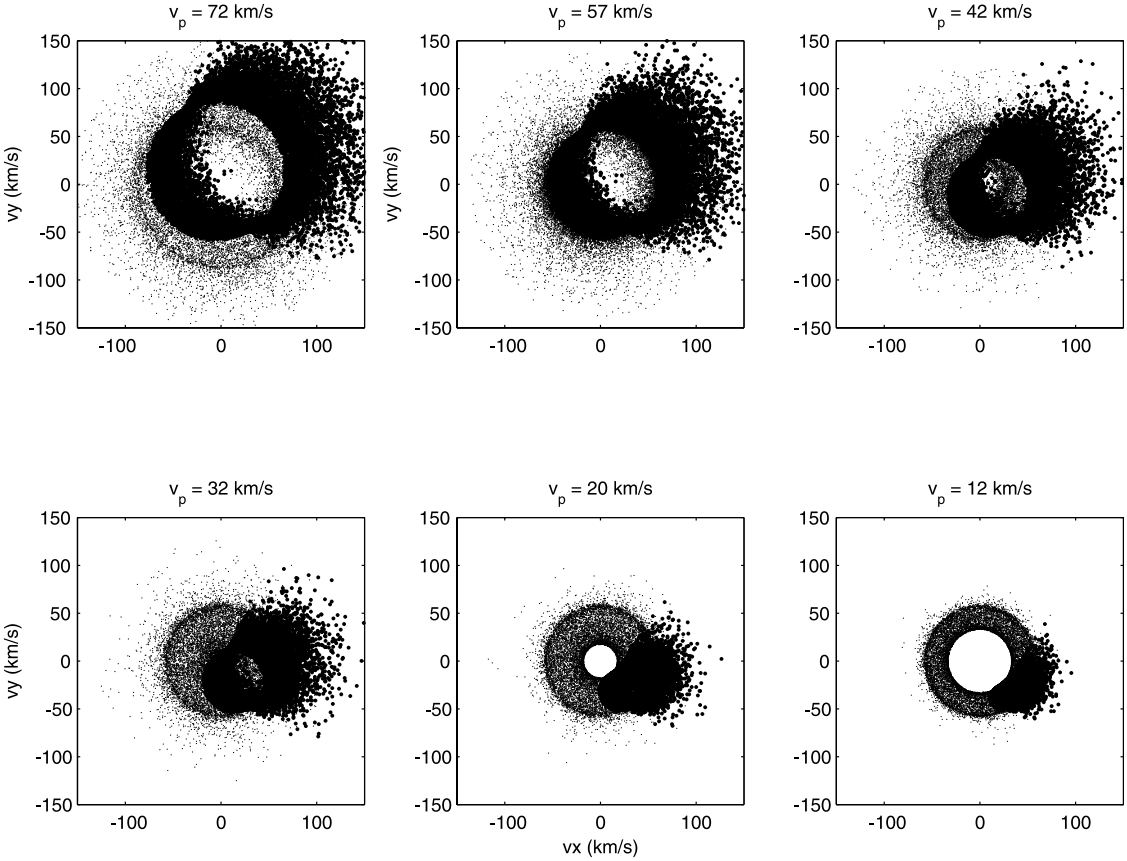

Figure 8. Gyrovelocity space plots of the ions for various pickup velocities. The small dots represent the ions in steady state after they have been accelerated by the corotation electric field during their final ion lifetime. The large dots are the ions before they were accelerated in this final stage. Note that if the large dots are plotted in the reference frame of the plasma flow into which they were added at Io (not the current corotating reference at their radial distance), they form ring shapes.

torus. It also moves the peak outward from Io's orbital distance. Ions have built up at the inner edge; however, the loading profile is not sufficient to build up enough ions to see a steep gradient. The outer edge is closer to Io than in the previous case, since the ions are moved out with greater speed. Velocity profile F is the same as profile D except moved across the x axis by $\sim$3.5 R_J. This puts the lowest velocities of the profile near the inner edge of the distribution, enabling particles to build up. The resulting inner torus gradient is very steep and, like case A, has bumps in the density profile. When the loading profile from the *Wang et al.* [2001] model is smoothed out, the bumps disappear, as shown in case G. Higher convective velocities also smooth out small density variations.

[15] Case F is compared to the A34 pass in Figure 11. The steepness of the inner boundary is well reproduced, as is the radial range of the density. As mentioned previously, the small peaks and valleys in the result of the F profile are due to the small peaks and valleys of the loading profile, which build up over time in the low convective velocity field and become more exaggerated. Unlike observations, the peak near Io is displaced outward from its observed location, indicating that in the real torus there is likely an inward motion of plasma at Io. The multiple density peak observed on A34 and other Galileo passes through the inner torus was not reproduced. If the density peak at the inner torus is the result of some large mass-loading event, then it is possible that the inner torus boundary gradient is generally not as steep and higher convective velocities would be more appropriate. Figure 12 shows several less steep ion radial profiles for cases H–J.

[16] While the *Wang et al.* [2001] model used sulfur monoxide exclusively, we will explore mass loading with sulfur dioxide and sulfur, other pickup ion species, which are observed to generate ion cyclotron waves in the torus. The ionization lifetime of sulfur compounds in the torus is less than several hours [*Smyth and Marconi*, 1998a], and as was shown by *Wang et al.* [2001], the choice of lifetimes for the Iogenic particle in its neutral stage of at least $\sim$25 min allows the neutralized ions sufficient time to reach the inner torus boundary. Use of a lifetime greater than this only serves to increase the density of the particle distribution and does not move the inner torus boundary. In the final ion stage of the model, since the ions do not experience any radial transport, the length of the final ion lifetime does not affect the radial locations of the density peak and the inner boundary or the overall shape of the radial density profile. In addition, decreasing the initial ion lifetime does not affect the distribution as long as the ion can complete one full gyration before being neutralized.

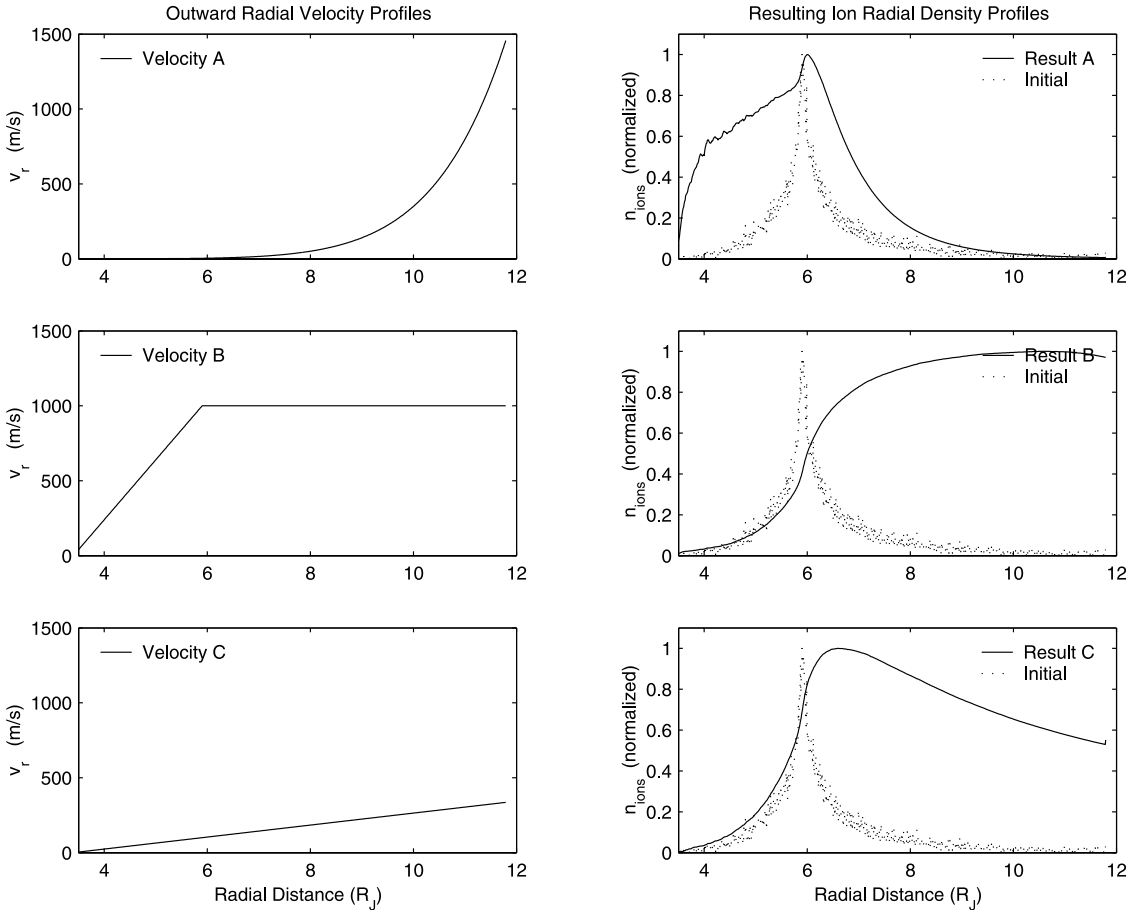

Figure 9. Convective velocity profiles A–C and the resulting normalized steady state ion radial distributions. The normalized initial distribution is shown with a dotted line. All cases use initial and loading density profiles derived from the *Wang et al.* [2001] model with pickup velocity equal to 57 km/s.

[17] Figure 13 compares the steady state neutral particle distribution for the cases of mass-loaded sulfur dioxide (m = 48 amu) and sulfur (m = 16 amu) under the same pickup conditions. While there are small, qualitative differences in the two distributions due to gyroradius effects, the overall distribution of mass-loaded particles is the same regardless of mass. Applying the same convective velocity profile as shown in case F to the sulfur or sulfur dioxide distribution results in the same steepened inner torus boundary that occurred with sulfur monoxide.

2.3. Other Considerations in the Structure of the Torus

[18] In the discussion in section 2.2, we implicitly assumed that the torus region is axisymmetric. If, in fact, there is a strong asymmetry in the magnetospheric electric field (corotational plus that imposed by the outer magnetosphere), then the differences in the observed radial location of the various density features between the passes could result from differing spacecraft trajectories. If so, the location of the steep density gradient in the inner torus on the various passes does not reflect a dynamically changing inner torus structure but rather a steady state. In order to discuss this possibility, Tables 1a–1c show Galileo's position during its passes through the torus during the J0 inbound and outbound passes and A34.

[19] When Galileo passed through the inner torus boundary on J0, it detected it at approximately 5 R_J, 4.75 $\mathrm{Lat_{III}}$, and −3 MLAT. On A34 it detected the inner torus boundary at approximately 4.7 R_J, −0.73 $\mathrm{Lat_{III}}$, and 0 MLAT. Models of the latitudinal structure of the Io torus [*Bagenal*, 1994; *Moncuquet et al.*, 2002] show an inner torus electron density structure with steep gradients and density peaks close to the centrifugal equator. These models only predict latitudinal structure in to 5 R_J, however, making comparison of the inner boundary data difficult. We presume that because of the confined latitudinal widths of the density peaks, Galileo was close to the centrifugal equator when it observed them on J0 and A34 and that the confined radial width of the peaks to within a tenth of a Jovian radius indicate that the ∼0.3 R_J difference in the observed locations of the inner boundary and density peaks cannot be fully accounted for by spacecraft trajectory. However, if we assume that the spacecraft did not necessarily fly through the most dense portions of the torus, then the heights of the density peaks are relative. If the torus structure is assumed to be the same on Voyager's inbound and outbound passes, then the variations in peak intensity and location are functions of the spacecraft trajectory. The Voyager data are difficult to interpret because there is no clear double-peak structure on the outbound pass; however, it does appear that the peaks vary by as much as ∼0.2 R_J in the

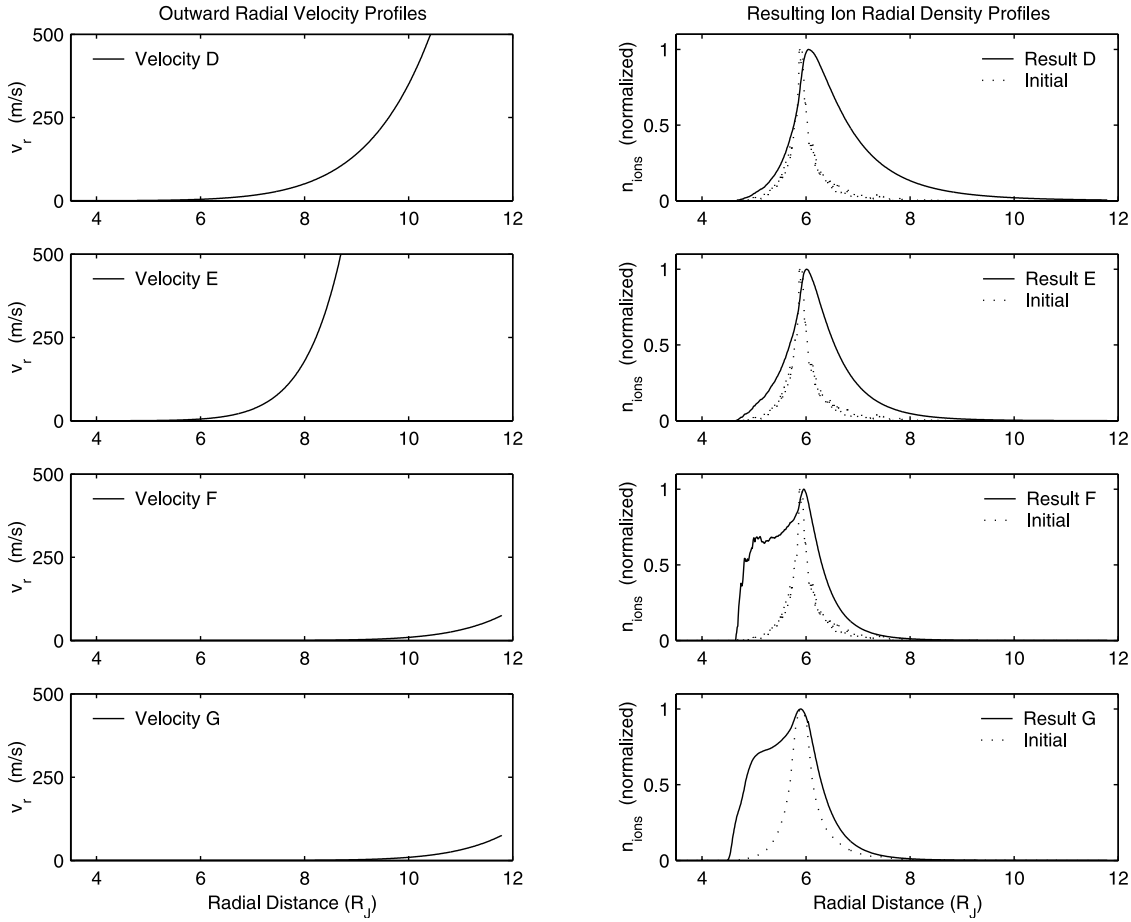

Figure 10. Convective velocity profiles D–G and the resulting normalized steady state ion radial distributions. The normalized initial distribution is shown with a dotted line. All cases use initial and loading density profiles derived from the *Wang et al.* [2001] model with pickup velocity equal to 20 km/s.

location of their detection. Thus the possibility exists that the difference between the J0 and A34 passes is a trajectory effect.

[20] Remote sensing of the torus suggests it varies its distance from Jupiter because of the effect of a dawn-dusk electric field across the magnetodisk. First identified by *Sandel and Broadfoot* [1982], the torus exhibits an east-west (or dawn-dusk) asymmetry where the dusk side is brighter (and hotter) than the dawn side. *Barbosa and Kivelson* [1983] explained this effect as the result of a dawn-dusk electric field resulting from the flow of magnetodisk plasma down the tail. This electric field shifts the orbits of the torus ions toward dawn, such that the torus is closer to Jupiter at the dawn ansa than at the dusk ansa. Observing the radial location of the brightest region of the torus at [S III] and [S II], *Dessler and Sandel* [1992] and *Schneider and Trauger* [1995] saw, in addition to a dawn-dusk asymmetry, a system III longitudinal (Lon_{III}) dependence. Ground-based observations of the Io torus "ribbon," the brightest region of the torus, associated with the density peak nearest Io, show that its location varies depending on its local time and longitude [*Bagenal et al.*, 1997]. If the changing location of the ribbon is an indicator of the changing location of other density features in the torus, then the inner boundary should be expected to vary its distance from Jupiter in a similar way.

[21] *Smyth and Marconi* [1998b] fit the sulfur emission observations of *Dessler and Sandel* [1992] and *Schneider and Trauger* [1995] in order to predict the location of the brightest region of the torus at the dusk and dawn ansae

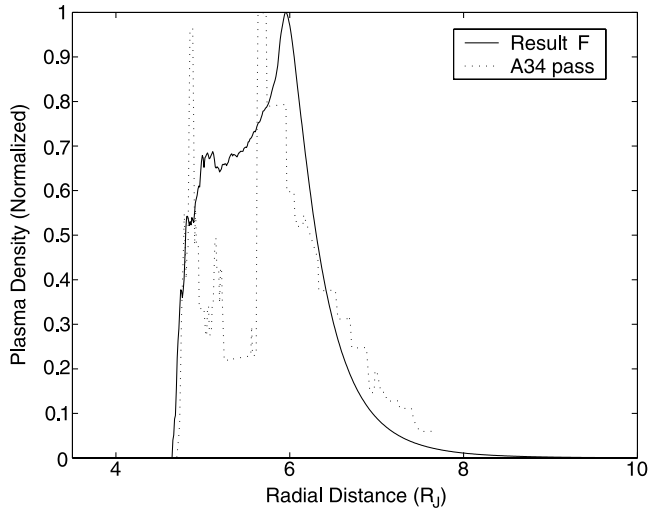

Figure 11. Comparison of the A34 and result of the F density profiles. A34 data are courtesy of D. A. Gurnett (private communication, 2003).

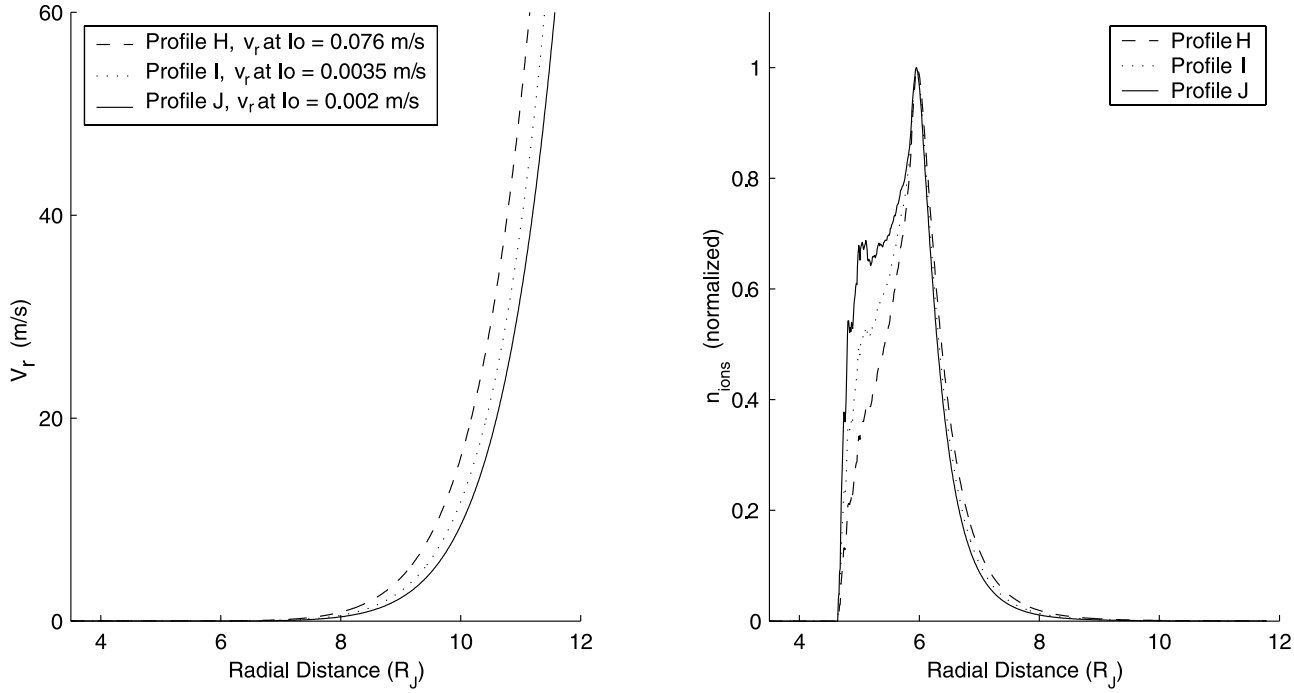

Figure 12. Convective velocity profiles H–J and the resulting normalized steady state ion radial distributions. The normalized initial distribution is shown with a dotted line. All cases use initial and loading density profiles derived from the *Wang et al.* [2001] model with pickup velocity equal to 20 km/s.

depending on Lon_{III}. For the cases of J0 and A34, with inner boundary crossings both at roughly the same local time near dusk (Table 2), the brightest region of the torus should be farther from Jupiter at 115° longitude on the A34 pass than 45° longitude on J0. However, *Smyth and Marconi* [1998b] predict that the whole torus structure, including density peaks, should be shifted closer to Jupiter on A34. While the east-west effect could exhibit a ~0.3 R_J difference in the

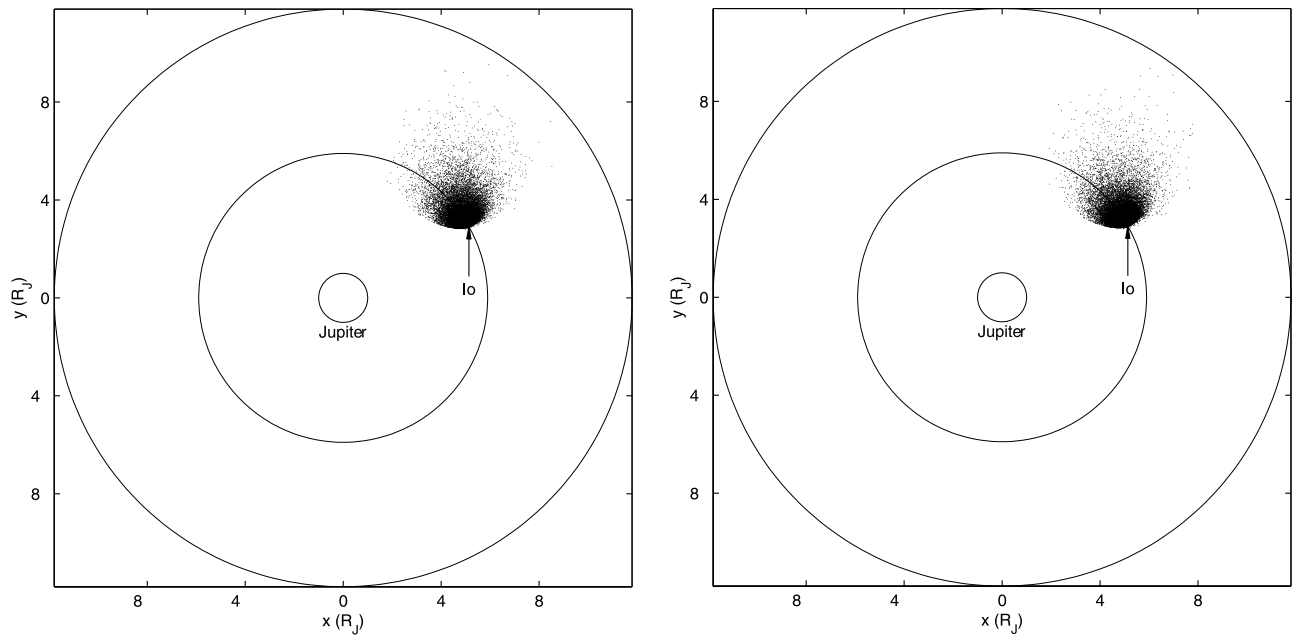

Figure 13. Comparison of the steady state particle distribution from the *Wang et al.* [2001] model for the cases of (left) sulfur dioxide and (right) sulfur mass loaded under the same conditions, with pickup velocity equal to 20 km/s. The distributions are very similar; any small differences are due to the differences in the gyroradii of these different mass particles. When subjected to the same outward convective velocities, they form the similarly shaped density profiles.

Table 1a. J0 (Inbound), 7 December 1995

	SCET[a]						
	1530	1600	1630	1700	1730	1800	1830
R,[b] R_J	7.60	7.21	6.83	6.45	6.08	5.72	5.37
Lon_{III}	209	223.9	238.5	252.6	266.3	279.4	291.9
Lat_{III}	−1.71	−1.43	−1.11	−0.75	−0.37	0.15	0.67
MLAT	7.81	7.47	6.59	5.33	3.82	2.24	0.71

[a]SCET is spacecraft event time.
[b]R is radial distance from Saturn in Jovian radii.

Table 1c. A34, 5 November 2002

	SCET						
	0000	0100	0200	0300	0400	0500	0530
R, R_J	8.71	7.82	6.88	5.91	4.90	3.85	2.82
Lon_{III}	348.37	21.10	52.89	83.24	111.18	134.66	148.62
Lat_{III}	−0.729	−0.738	−0.746	−0.749	−0.738	−0.692	−0.636
MLAT	−8.71	−10.34	−8.98	−5.35	−0.88	2.99	5.17

radial location of the torus density structure [*Dessler and Sandel*, 1992], it does not explain the difference on the J0 and A34 passes.

[22] If the large density peak nearest to Io is directly associated with the ribbon, then it may be a better indicator of the system III periodicity in the torus. The location of Galileo and Voyager during their detection of the near Io peak are shown in Table 3. As predicted by *Smyth and Marconi* [1998b] and as was observed by Voyager, the location of the ribbon should be closer to Jupiter on the Voyager 1 outbound trajectory than on its inbound one. However, the near-Io peak observed on J0 is farther from Jupiter than was observed on A34, opposite of what is predicted. This inconsistency for the J0 and A34 passes may be due to other magnetospheric conditions or to latitudinal variations in the torus structure. It is also possible that variations in the whole torus structure may not be predicted by the location of the ribbon or that the torus does not always exhibit system III longitudinal periodicity. *Nozawa et al.* [2004] indicate that although the torus does exhibit a system III periodicity in the short term, it does not do so over years. Since the J0 and A34 passes were 7 years apart, they should not necessarily be expected to exhibit a system III periodicity. By contrast, the Voyager inbound and outbound passes, which occurred within hours of each other, should show a torus structure correlated with Lon_{III}.

3. Conclusions

[23] Ion pickup in the Io atmosphere can occur in a plasma that is slowed relative to its corotation velocity. The model by *Wang et al.* [2001] considers ion pickup into a corotating flow, $\mathbf{v}_{cor}$ = 74 km/s, from a velocity equal to Io's orbital velocity, $\mathbf{v}_{Io}$ = 17 km/s. In this 57 km/s pickup velocity case the inner torus boundary is located at ~3.5 R_J. For an inner torus boundary at ~4.7 R_J, as is consistent with Galileo pass A34 observations, the plasma flow near Io would need to be slowed to 37 km/s ($\mathbf{v}_{pickup}$ = 20 km/s); for an inner edge at 5 R_J, as shown in pass J0, the plasma would be slowed to 29 km/s ($\mathbf{v}_{pickup}$ = 12 km/s). Galileo observed plasma flows decelerated to several kilometers per second relative to Io's orbital velocity as well as those accelerated faster than corotation.

[24] As expected, if the pickup velocity is increased from 57 km/s, the average gyrokinetic energy in each radial bin also increases. However, for decreasing pickup velocity, there is an unexpected effect. Because of the multiple stages of acceleration in the model, higher final gyrokinetic energies are favored for particles with lower pickup velocities at Io. Low-temperature gaps form for particles with pickup velocities less than about half the corotation pickup velocity. This affects the average energies such that as pickup velocity is lowered, the average gyrokinetic energy per radial bin actually increases. Modeled velocities are higher than the observations because the model does not include any ion cooling and it only considers sulfur monoxide particles. SO^+ will dissociate into its constituent ions, decreasing the average temperature per ion.

[25] The inclusion of an outward radial convection of the *Wang et al.* [2001] simulated ion distribution with 20 km/s pickup velocity successfully reproduced the steep inner edge of the inner torus observed on the A34 pass. The outer torus density gradient was also generally reproduced, but the multiple density peaks were not, and the density peak near Io was moved outward in the torus instead of inward. We have not included the fluid dynamics of the slowed flow near Io in our calculations, however. A slowed flow will have a different force balance than the nearby fully corotating flow and could deviate from strictly longitudinal motion near Io.

[26] We also considered mass-loaded sulfur in our model and showed that the overall distribution of particles was similar to that of mass-loaded sulfur monoxide. The location of the inner torus boundary is independent of mass and is changed only by altering the pickup velocity or the lifetimes of the particles. When these steady state distributions of different mass particles from the *Wang et al.* [2001] model are convected outward with the same velocities, they produce similarly shaped radial density profiles. The exact form of the outward convective velocity profile is uncertain,

Table 1b. J0 (Outbound), 7 December 1995 to 8 December 1995

	SCET				
	2330	0000	0030	0100	0130
R, R_J	4.36	4.59	4.87	5.18	5.50
Lon_{III}	20.4	29.8	40.0	51.36	63.51
Lat_{III}	5.45	5.24	4.95	4.62	4.28
MLAT	−4.15	−4.27	−4.17	−3.74	2.89

Table 2. Estimated Location of Io Inner Torus Boundary

Pass	R/R_J (Inner Boundary)	Lon_{III}	LT
J0 (out)	5	45	2000
A34	4.7	115	1900
V1 (in)[a]	4.9	250	1845
V1 (out)[a]	5.3	300	2130

[a]Estimates for the location of the inner boundary for Voyager 1 may be incorrect because the spacecraft did not fly far enough into the inner torus. These values assume that Voyager 1 did actually cross the inner boundary.

Table 3. Estimated Location of the Near-Io Peak

Pass	R/R_J (Near-Io Peak)	Lon_{III}	LT
J0 (in)	5.9	270	2000
A34	5.7	90	1830
V1 (in)	5.7	200	1630
V1 (out)	5.5	310	2145

because although our model shows that velocities should increase with radial distance, as is consistent with observations [*Russell et al.*, 2000; *Intriligator and Miller*, 1982], it is highly simplified and ignores many important transport mechanisms in the torus. Inward convection of plasma also occurs, as evidenced by the location of the density peak near Io, as well as diffusive plasma processes in the inner and outer torus [*Herbert*, 1996]. The net motion of the plasma, however, will be outward, as centrifugal forces act across the entire torus and are not be overwhelmed by plasma pressure of the cold inner torus.

[27] An apparent discrepancy between our model and the data is the inward displacement of the inner boundary location by $\sim$0.3 R_J between the J0 pass and the A34 pass, 7 years later. Outward radial convection certainly cannot account for this motion. A highly efficient mass-loading event would have had to occur between the time of J0 and A34 that produced a new cold density region inside the J0 peak. Such an event could have been observed in August 1999 both by ground telescopes and Galileo. *Russell et al.* [2001], interpreting the fluxes of energetic particles detected by the star sensor on Galileo, believe a large mass-loading event took place either during or just before the Galileo C22 pass on 11 August.

[28] Also worth noting is the change in the configuration of the torus if the magnetosphere lost its outer magnetodisk and returned to a near-potential field state. If mass loading ceased and the magnetosphere were emptied of ions, the field lines near Io would move inward only 0.4 *Rj* (Figure 14). If the part of the inner Io torus that is not dynamically significant to the magnetodisk remained, it could also move this far.

[29] It is possible that the differences in the torus structure observed between the Galileo passes are due to the spacecraft trajectory. Since the torus exhibits a latitudinal structure with steep gradients at varying radial distances in the inner torus, the spacecraft's position could be very important in interpreting its results. The Voyager inbound and outbound passes, which saw $\sim$0.2 R_J differences in the radial location of features, indicate the possibility that the differences between J0 and A34 are trajectory-related. However, models of the inner torus latitudinal density structure only reach in to 5 R_J [*Bagenal*, 1994; *Moncuquet et al.*, 2002], making analysis of the A34 data difficult.

[30] The dawn-dusk electric field in the torus could also be responsible for a $\sim$0.3 R_J shift in torus structure [*Dessler and Sandel*, 1992]. This shift is predicted to also depend on system III longitude [*Smyth and Marconi*, 1998b]; however,

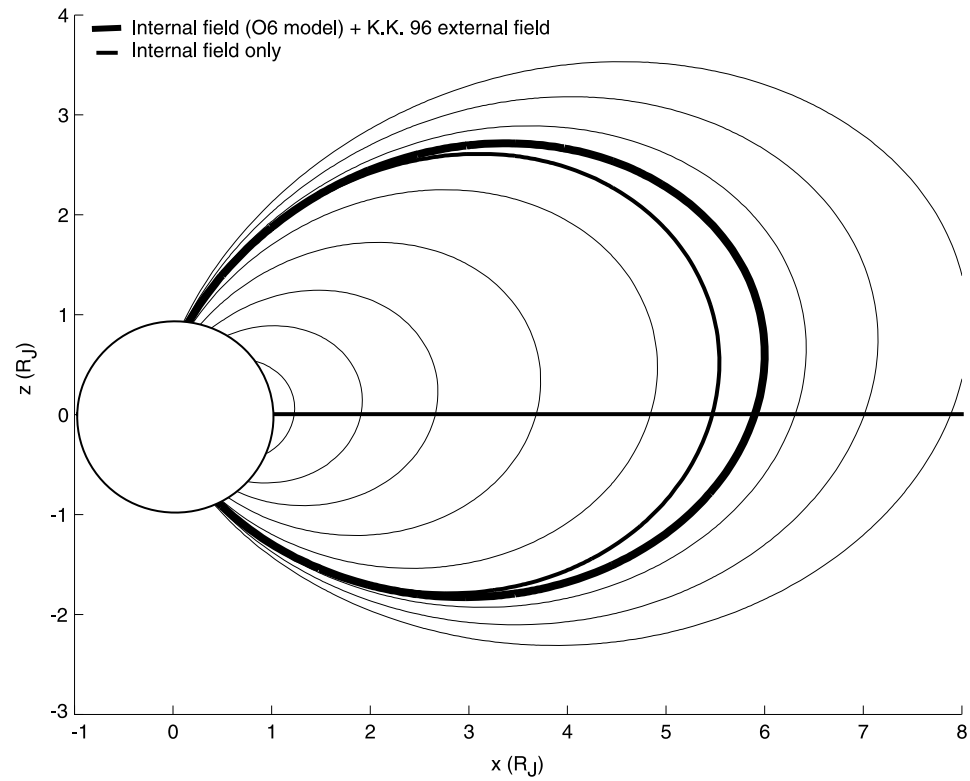

Figure 14. Modeled field lines of Jupiter's magnetic field. The thickest line shows the field line, which intersects the equator at Io's orbital distance of 5.9 R_J using both the internal field model, O6, and the external field model, KK 96 [*Khurana*, 1997]. If the external currents are removed, this field line moves inward and intersects at 5.47 R_J (middle thickness) Plot is courtesy of Z. J. Yu (private communication, 2004).

since the shift detected between J0 and A34 is opposite to predictions, it is possible that the torus does not exhibit a system III periodicity over years. *Herbert and Sandel* [2000] note the complications in observing system III dependence of UV emissions from the torus due to system IV fluctuations, and *Nozawa et al.* [2004] predict that while the torus may exhibit system III periodicity over short timescales, it does not do so over years; rather, it shows a system IV periodicity. Thus the differences between the inner boundary of the Io inner torus observed by Galileo on the J0 and A34 orbits are difficult to explain by the hypothesized spatial asymmetries in magnetospheric convection. It is possible that the differences indicate temporal variations in the mass-loading rate at Io or in the magnetospheric configuration.

[31] **Acknowledgments.** This work was supported by the National Aeronautics and Space Administration under research grant NAG 5-12022.
[32] Shadia Rifai Habbal thanks all the referees for their assistance in evaluating this paper.

References

Bagenal, F. (1994), Empirical model of the Io plasma torus: Voyager measurements, *J. Geophys. Res.*, *99*, 11,043–11,062.
Bagenal, F., F. J. Crary, A. I. F. Stewart, N. M. Schneider, D. A. Gurnett, W. S. Kurth, L. A. Frank, and W. R. Paterson (1997), Galileo measurements of plasma density in the Io torus, *Geophys. Res. Lett.*, *24*, 2119–2122.
Barbosa, D. D., and M. G. Kivelson (1983), Dawn-dusk electric field asymmetry of the Io plasma torus, *Geophys. Res. Lett.*, *10*, 210–213.
Dessler, A. J., and B. R. Sandel (1992), System III variations in the apparent distance of Io plasma torus from Jupiter, *Geophys. Res. Lett.*, *19*, 2099–2103.
Frank, L. A., and W. R. Paterson (2000), Return to Io by the Galileo spacecraft: Plasma observations, *J. Geophys. Res.*, *105*, 25,363–25,378.
Frank, L. A., and W. R. Paterson (2001), Passage through Io's ionospheric plasmas by the Galileo spacecraft, *J. Geophys. Res.*, *106*, 26,209–26,224.
Frank, L. A., and W. R. Paterson (2002), Plasmas observed with the Galileo spacecraft during its flyby over Io's northern polar region, *J. Geophys. Res.*, *107*(A8), 1220, doi:10.1029/2002JA009240.
Frank, L. A., W. R. Paterson, K. L. Ackerson, V. M. Vasyliunas, F. V. Coroniti, and S. J. Bolton (1996), Plasma observations at Io with the Galileo spacecraft, *Science*, *274*, 394–395.
Herbert, F. (1996), A simple transport model for the Io plasma torus "ribbon", *Geophys. Res. Lett.*, *23*, 2875–2878.
Herbert, F., and B. R. Sandel (2000), Azimuthal variation of ion density and electron temperature in the Io plasma torus, *J. Geophys. Res.*, *105*, 16,035–16,052.
Intriligator, D. S., and W. D. Miller (1982), First evidence for a Europa plasma torus, *J. Geophys. Res.*, *87*, 8081–8090.
Khurana, K. K. (1997), Euler potential models of Jupiter's magnetospheric field, *J. Geophys. Res.*, *102*, 11,295–11,306.
Moncuquet, M., F. Bagenal, and N. Meyer-Vernet (2002), Latitudinal structure of outer Io plasma torus, *J. Geophys. Res.*, *107*(A9), 1260, doi:10.1029/2001JA900124.
Nozawa, H., H. Misawa, S. Takahashi, A. Morioka, S. Okano, and R. Sood (2004), Long-term variability of [SII] emissions from the Io plasma torus between 1997 and 2000, *J. Geophys. Res.*, *109*, A07209, doi:10.1029/2003JA010241.
Russell, C. T., M. G. Kivelson, K. K. Khurana, and D. E. Huddleston (2000), Circulation and dynamics in the Jovian magnetosphere, *Adv. Space Res.*, *26*, 1671–1676.
Russell, C. T., P. D. Fieseler, D. Bindshadler, Z. J. Yu, S. P. Joy, K. K. Khurana, and M. G. Kivelson (2001), Large-scale changes in the highly energetic charged particles in the region of the Io torus, *Adv. Space Res.*, *28*, 1495–1500.
Sandel, B. R., and A. L. Broadfoot (1982), Io's hot plasma torus: A synoptic view from Voyager, *J. Geophys. Res.*, *87*, 212–218.
Schneider, N. M., and J. T. Trauger (1995), The structure of the Io torus, *Astrophys. J.*, *450*, 450–462.
Smyth, W. H., and M. L. Marconi (1998a), An initial look at the Iogenic SO_2^+ source during the Galileo flyby of Io, *J. Geophys. Res.*, *103*, 9083–9089.
Smyth, W. H., and M. L. Marconi (1998b), An explanation for the east-west asymmetry of the Io plasma torus, *J. Geophys. Res.*, *103*, 9091–9100.
Wang, Y., C. T. Russell, and J. Raeder (2001), The Io mass-loading disk: Model calculations, *J. Geophys. Res.*, *106*, 26,243–26,260.

M. M. Cowee and C. T. Russell, Institute of Geophysics and Planetary Physics, University of California, Los Angeles, Los Angeles, CA 90095, USA. (mcowee@igpp.ucla.edu)
D. A. Gurnett, Department of Physics and Astronomy, University of Iowa, Iowa City, IA 52242, USA.
Y. L. Wang, Space and Atmospheric Sciences Group, Los Alamos National Laboratory, Los Alamos, NM 87545, USA.